

# Shear viscosity of classical fields in scalar theory

Hidefumi Matsuda,<sup>1</sup> Teiji Kunihiro,<sup>1,2</sup> Akira Ohnishi,<sup>2</sup> and Toru T. Takahashi<sup>3</sup>

<sup>1</sup>*Department of Physics, Faculty of Science, Kyoto University, Kyoto 606-8502, Japan*

<sup>2</sup>*Yukawa Institute for Theoretical Physics, Kyoto University, Kyoto 606-8502, Japan*

<sup>3</sup>*Gunma National College of Technology, Gunma 371-8530, Japan*

We investigate the shear viscosity of classical scalar fields in the  $\phi^4$  theory on a lattice by using the Green-Kubo formula. Equilibrium expectation value of the time correlation function of the energy-momentum tensor is evaluated as the ensemble average of the classical field configurations, whose time evolution is obtained by solving the classical equation of motion starting from the initial condition in thermal equilibrium. It is found that there are two distinct damping time scales in the time correlation function, which is found to show damped oscillation behavior in the early stage around a slow monotonous decay with an exponential form, and the slow decay part is found to dominate the shear viscosity. This kind of slow decay is also known to exist in the molecular dynamics simulation, then it may be a generic feature of dense matter. The obtained shear viscosity is smaller than the perturbative estimate in the quantum theory which may well describe the hard sector, and suggests a strong coupling feature of the classical field theory which in turn may well describe the infrared dynamics of the whole quantum theory.

## I. INTRODUCTION

Classical fields have been proven useful in describing various physical systems which have actually quantum nature, such as the condensate of Bose gases [1], inflation in the early universe [2], nuclear structure [3], and gluon fields in heavy-ion collisions [4, 5]. They can be used to obtain the ground states, for example, of Bose gases by using the Gross-Pitaevskii equation [1] and those of nuclei in the relativistic mean field theory [3]. Classical field theory can be also utilized to understand the dynamical evolution of the system [2, 4, 5]. In dynamical evolution of a quantum system, particles can be created by a coupling with the classical field, and its creation and their mutual collisions produce entropy and lead to eventual thermalization. Furthermore, it has been shown that the dynamics of the classical field itself is responsible for entropy production in a semiclassical approximation and thus play a significant role in the realization of an approximate local thermal equilibrium so that the hydrodynamical description of the time-evolution afterward becomes valid in the case of Yang-Mills field [6]. The classical field dynamics and its possible relevance to entropy production is considered as one of the key ingredients for a hydrodynamical description of a quantum system, then it would be intriguing to explore the properties of nonequilibrium processes as well as equilibrium statistical physics of classical fields. As far as we are aware of, it seems that systematic investigations of nonequilibrium properties of classical fields have not been done so far, except for few exceptions if exist. Taking account of the possible role of classical fields in thermalization, it is natural to expect that the classical field has its own viscosity [7]. The Green-Kubo formula, shown later in Eq. (5), tells us that the shear viscosity can be obtained from the integral of the time correlation function of the energy-momentum tensor,  $C_{12}(t)$  to  $t = \infty$ . Since the Green-Kubo formula is obtained from the linear response theory and should be valid independent of the theoretical framework, it is pos-

sible to obtain the shear viscosity provided by classical fields from the thermal average of  $C_{12}(t)$ .

In this work, we discuss the shear viscosity of the classical field in the  $\phi^4$  theory using the Green-Kubo formula. In order to make thermalized initial states, we utilize the Langevin equation composed of streaming, diffusion and stochastic force (latter two are collectively called the Langevin terms) to generate configurations in thermal equilibrium; the achievement of thermal equilibrium is checked by examining the equipartition of energy. Once the thermal equilibrium is realized, the Langevin terms are switched off and the time evolution of the system is solely governed by the intrinsic dynamics of the  $\phi^4$  theory. Then we calculate  $C_{12}(t)$ .

One of the purposes of the present work is a detailed analysis of the time correlation of the classical energy-momentum tensor  $C_{12}(t)$ , which turns out to exhibit rich phenomena beyond naïve expectation such as a simple damped oscillation. In fact, such an analysis is necessary to extract the viscosity in a physically meaningful way. It contains two main components; a fast damped oscillation seen in the early stage and a slow monotonous decay with an exponential form. We also make a detailed analysis of the spectral function which contain interesting physics of the excitation modes of the system. The decay rates of these two components are different by two or three orders in magnitude, and the slow decay part dominates the integral of  $C_{12}(t)$ . We show that subtraction of the exponential term is necessary to make the integration to  $t = \infty$  in the Green-Kubo formula well-defined. The obtained shear viscosity is found to be smaller than the value in perturbative calculations based on quantum field theory at finite temperature. According to the rarefied gas argument, the shear viscosity is proportional to the mean free path, then the small shear viscosity suggests a shorter mean free path in the classical field theory than that in perturbative calculations. This may be because the energy density spreads over the lattice in the classical field theory, and each momentum mode always interacts

with other modes. Then collective long-lived modes may appear as in hydrodynamics.

*Subtlety:* We should remember that there is a subtlety in discussing thermalization and equilibrium using classical fields. Classical field theory is an effective theory of low momentum modes of quantum systems. In the equilibrium of classical fields, an approximate equipartition of energy holds and each mode has the energy around the temperature. Thus the distribution of massless particles obeys the Rayleigh-Jeans law, which agrees with the Bose-Einstein distribution at low momenta, and the energy density of the classical field is divergent in the continuum limit. Therefore we should set the ultraviolet cutoff scale around the temperature. Another way would be to take account of the coupling with particles, which is beyond the scope of this article.

This paper is organized as follows. In Sec. II, we first explain the lattice formulation of the classical field in the  $\phi^4$  theory, the classical field ensemble, and the Green-Kubo formula for the shear viscosity. We also discuss the Langevin terms, which promote thermalization, and the equipartition nature in the equilibrium of the classical fields. In Sec. III, we show the numerical results of the time correlation of the energy-momentum tensor and its Fourier spectrum. The shear viscosity is obtained from the  $\omega \rightarrow 0$  limit of the Fourier spectrum. We also discuss the coupling dependence of the shear viscosity. In Sec. IV, we summarize our work.

## II. CLASSICAL SCALAR FIELD AND ITS SHEAR VISCOSITY

### A. Classical Scalar Field Theory on Lattice

We consider the  $\phi^4$  theory, where the Lagrangian is given as

$$\mathcal{L} = \frac{1}{2} \partial_\mu \phi \partial^\mu \phi - \frac{1}{2} m^2 \phi^2 - \frac{\lambda}{24} \phi^4. \quad (1)$$

On a  $L^3$  lattice, the Hamiltonian is given by

$$H = \frac{1}{2} \sum_{\mathbf{x}} \left[ \pi^2(\mathbf{x}) + (\partial_i \phi(\mathbf{x}))^2 + m^2 \phi(\mathbf{x})^2 + \frac{\lambda}{12} \phi^4(\mathbf{x}) \right], \quad (2)$$

where  $(\phi(\mathbf{x}), \pi(\mathbf{x}) = \dot{\phi}(\mathbf{x}))$  are the canonical variables and  $\partial_i$  denotes the forward difference operator in the  $i$ -th direction, i.e.  $\partial_i \phi(\mathbf{x}) = \phi(\mathbf{x} + \hat{e}^i) - \phi(\mathbf{x})$ . We take all quantities normalized by the lattice spacing  $a$  throughout this article.

We discuss the evolution of the scalar field in the classical field approximation, where the field variables  $(\phi(\mathbf{x}), \pi(\mathbf{x}))$  are regarded as  $c$ -numbers. Instead of taking account of fluctuations of the field operators in the evolution in each classical field configuration, statistical fluctuations are taken into account by using the classical

field ensemble as described later. Then the above Hamiltonian is regarded as a classical Hamiltonian, which gives the classical equation of motion,

$$\dot{\phi}(\mathbf{x}) = \frac{\partial H}{\partial \pi(\mathbf{x})}, \quad \dot{\pi}(\mathbf{x}) = -\frac{\partial H}{\partial \phi(\mathbf{x})}. \quad (3)$$

We define the off-diagonal matrix elements of the energy-momentum tensor of scalar fields on the lattice as

$$T_{ij} \equiv (\partial_i^c \phi(\mathbf{x})) (\partial_j^c \phi(\mathbf{x})) \quad (i \neq j). \quad (4)$$

Here we adopt the central difference,  $\partial_i^c \phi(\mathbf{x}) = [\phi(\mathbf{x} + \hat{e}^i) - \phi(\mathbf{x} - \hat{e}^i)]/2$ . With this prescription,  $\partial_i^c \phi(\mathbf{x})$  is located in the same space-time point as  $\phi(\mathbf{x})$  and the matrix element becomes more symmetric in the space directions. Then the central difference  $\partial_i^c$  is found to give a better definition of the energy-momentum tensor than the forward difference operator  $\partial_i$ .

### B. Green-Kubo Relation

We evaluate the shear viscosity of the classical field by using the Green-Kubo formula which is a powerful relation in the linear response theory[8].

$$\eta = \lim_{\omega \rightarrow 0} \frac{1}{T} \int_0^\infty dt e^{i\omega t} C_{12}(t), \quad (5)$$

$$C_{12}(t) = V \langle \tau_{12}(t) \tau_{12}(0) \rangle_{\text{eq}}, \quad (6)$$

$$\tau_{12}(t) \equiv \frac{1}{V} \int d^3x \tau_{12}(\mathbf{x}, t), \quad (7)$$

where  $T$  and  $V$  denote temperature and volume, respectively,  $\tau_{12}(t)$  is the space-averaged off-diagonal matrix element of the energy-momentum tensor, and  $\langle \cdots \rangle_{\text{eq}}$  represents the expectation value in equilibrium.

In the long time-difference limit  $t \rightarrow \infty$ , the correlation disappears and  $C_{12}(t)$  is expected to become 0.

$$C_{12}(t) = V \langle \tau_{12}(t) \tau_{12}(0) \rangle_{\text{eq}} \xrightarrow{t \rightarrow \infty} V \langle \tau_{12}(0) \rangle_{\text{eq}}^2 = 0.$$

The final equality is expected from the isotropy of thermal systems. Thus when the correlation disappears faster than  $1/t$ , the integral in Eq. (5) converges to a finite value. In actual calculations, the correlation has a long tail and it is not easy to obtain the converged integral. As demonstrated later, we find that it is possible to evaluate the integral to infinity safely by subtracting the slowly decreasing exponential function and adding the exponential contribution separately.

### C. Equilibrium in Classical Field Ensemble

In the Green-Kubo formula, we need the equilibrium expectation value of the time correlation of the energy-momentum tensor. We here obtain the equilibrium expectation value by using configurations in the classical

field ensemble. We prepare  $N_{\text{conf}}$  initial classical field configurations in equilibrium. Then we regard the average of observables in this ensemble as the expectation values in classical equilibrium,

$$\langle \mathcal{O} \rangle_{\text{eq}} \simeq \frac{1}{N_{\text{conf}}} \sum_{i=1}^{N_{\text{conf}}} \mathcal{O}_i, \quad (8)$$

where  $\langle \mathcal{O} \rangle_{\text{eq}}$  is the expectation value of the observable  $\hat{\mathcal{O}}$ ,  $N_{\text{conf}}$  is the number of classical field configurations, and  $\mathcal{O}_i$  is the observable in the  $i$ -th configuration.

In order to obtain many equilibrium classical field configurations efficiently, we introduce the artificial Langevin terms in the thermalization stage. In the  $\phi^4$  theory, it takes a long time for the system to equilibrate especially at low  $T$  or  $\lambda$ , then a large computational resource is required to prepare a large number of equilibrium configurations. By introducing the Langevin terms, thermalization is hastened. We add the Langevin terms, combination of the diffusion and stochastic forces, to the right hand side of the equation of motion for  $\pi(x)$ ,

$$\dot{\pi}(x) = -\frac{\partial H}{\partial \phi(x)} - \gamma \pi(x) + R(x), \quad (9)$$

where  $\gamma$  is the diffusion coefficient and  $R(x)$  represents the fluctuation, which is assumed to obey a Gaussian distribution function, namely the white noise. The strength of the fluctuation is determined by the Einstein relation,

$$\langle R(x)R(x') \rangle = 2\gamma T \delta(t - t') \delta_{\mathbf{x}, \mathbf{x}'}, \quad (10)$$

where  $T$  is the temperature.

When equilibrium is reached, classical field configurations are distributed according to the Boltzmann weight. The partition function of the classical field on the lattice is given as

$$\begin{aligned} \mathcal{Z} &= \int \mathcal{D}\pi \mathcal{D}\phi \exp(-H/T) \\ &= \int \mathcal{D}\pi \exp\left(-\frac{1}{2T} \sum_{\mathbf{x}} \pi^2(\mathbf{x})\right) \int \mathcal{D}\phi e^{-H_\phi/T} \\ &= \prod_{\mathbf{k}} \left[ \int d\pi(\mathbf{k}) e^{-|\pi(\mathbf{k})|^2/2T} \right] \int \mathcal{D}\phi e^{-H_\phi/T}, \quad (11) \end{aligned}$$

where  $\mathbf{k}$  denotes the lattice momentum  $\mathbf{k} = 2\pi(n_x, n_y, n_z)/L$  ( $n_i = 0, 1, \dots, L-1$ ),  $\pi(\mathbf{k}) = \sum_{\mathbf{x}} \pi(\mathbf{x}) e^{-i\mathbf{k} \cdot \mathbf{x}} / \sqrt{L^3}$  is the Fourier transform of  $\pi(\mathbf{x})$ , and  $H_\phi$  is the Hamiltonian terms containing  $\phi$ .

Note that  $\pi(\mathbf{k})$  is complex in general and  $\pi(\mathbf{k})$  and  $\pi(-\mathbf{k})$  satisfies  $\pi(-\mathbf{k}) = \pi(\mathbf{k})^*$ , then the integral should be regarded to be  $d\pi(\mathbf{k})d\pi(-\mathbf{k}) = 2d\text{Re}\pi(\mathbf{k})d\text{Im}\pi(\mathbf{k})$ . Only in those cases with all the momentum components being 0 or  $\pi$ ,  $\pi(\mathbf{k})$  is real.

Since the Hamiltonian is quadratic in  $\pi(\mathbf{x})$  as well as in  $\pi(\mathbf{k})$ , the expectation values in equilibrium should be given as

$$\langle \pi(\mathbf{x})^2 \rangle_{\text{eq}} = T, \quad \langle |\pi(\mathbf{k})|^2 \rangle_{\text{eq}} = T. \quad (12)$$

Thus we can measure the temperature of classical equilibrium system from the expectation values of  $\pi(\mathbf{x})^2$  or  $|\pi(\mathbf{k})|^2$ , where the expectation value does not depend on the position and the momentum. In section III B, we check this relation.

#### D. Scaling property

In actual calculations, we concentrate on the time evolution of classical fields at  $m = 0$ , where equation of motion has the scaling property. The equation of motion, Eqs. (3) with  $m = 0$ , is invariant under the transformation,

$$\phi \rightarrow \phi/\sqrt{\alpha}, \quad \pi \rightarrow \pi/\sqrt{\alpha}, \quad \lambda \rightarrow \alpha\lambda. \quad (13)$$

Then the phase space trajectories are the same with this transformation, which is referred to as the  $\lambda$  deformation hereafter.

The  $\lambda$  deformation results in

$H_\lambda \rightarrow H_{\alpha\lambda}/\alpha$ , with  $H_\lambda$  being the Hamiltonian with the coupling  $\lambda$ , and the temperature defined above can be regarded as

$$T_\lambda = \langle \pi_x^2 \rangle_\lambda = \alpha \langle \pi_x^2 \rangle_{\alpha\lambda} = \alpha T_{\alpha\lambda}. \quad (14)$$

By using the  $\lambda$  deformation, the time correlation function and the shear viscosity at a given  $(\lambda, T)$  are found to be related with those having the same  $\lambda T$  value as,

$$C_{12}(t; \lambda, T) = \alpha^2 C_{12}(t; \alpha\lambda, T/\alpha), \quad (15)$$

$$\eta(\lambda, T) = \alpha \eta(\alpha\lambda, T/\alpha). \quad (16)$$

Then it is enough to vary  $\lambda$  and to keep  $T$  fixed in order to evaluate  $C_{12}(t)$  and  $\eta$  at various combinations of  $\lambda$  and  $T$ .

#### E. Momentum Cutoff

Thermally equilibrated classical fields obey the the Rayleigh-Jeans law, and the energy density is divergent in the continuum limit,  $a^{-1} \rightarrow \infty$ . When we consider classical field theories around the equilibrium, we need to set the ultraviolet momentum cutoff appropriately. As a momentum cutoff, we set the lattice spacing as  $a^{-1} = \mathcal{O}(T_{\text{phys}})$ . For example, in massless free classical field theories on the lattice, the energy per degrees of freedom agrees with the lattice temperature  $T$ , then we find  $\varepsilon = E/V = T$  for a one-component scalar field theory. The lattice energy density and the temperature are related with those in the physical unit as  $\varepsilon = a^4 \varepsilon_{\text{phys}}$  and  $T = a T_{\text{phys}}$ , then we find that  $\varepsilon_{\text{phys}}$  is proportional to  $T_{\text{phys}}^4$  as the Stefan-Boltzmann law implies.

In the later discussions, we set  $a^{-1} = T_{\text{phys}}/T$  and take  $T = \mathcal{O}(1)$ .

Specifically, we adopt  $T = 1$  in the actual numerical calculations, and use the  $\lambda$  deformation to evaluate the shear viscosity in the physical unit, as we will discuss in Sec. III E and Appendix D.

### III. NUMERICAL RESULTS

#### A. Calculation Setup

In actual calculations, we concentrate on the case with  $m = 0$ , where the equation of motion is invariant under the  $\lambda$  deformation. The coupling is chosen to be  $\lambda = 0.5, 1, 3, 5, 10$  and  $30$ . The calculations are performed with the three different lattice sizes  $L = 16, 32$  and  $64$ , and we mainly show the results with  $L = 32$ . Equilibrium classical field configurations are generated by introducing the Langevin terms with  $\gamma = 0.1$ . Time evolution with the Langevin terms is calculated with a fixed lattice temperature  $T = 1$  for a duration of  $t_{\text{eq}} = 1/\gamma$ , where we have confirmed that classical equilibrium is reached. After preparing  $N_{\text{conf}} = 1000$  classical field equilibrium configurations for each value of  $\lambda$ , we perform the time evolution calculation without the Langevin terms until  $t = 10^4/\lambda^2$ . The time evolution is calculated in the leap-frog scheme with the time step of  $\Delta t = 0.01$ .

#### B. Examination of Equilibrium

We first check that classical equilibrium is reached correctly by using the classical equilibrium relation in Eq. (12) at various frequencies. Thermalization process with the Langevin terms is discussed in Appendices A and B.

In Fig. 1, we show  $\langle |\pi(t, \mathbf{k})|^2 \rangle_{\text{eq}}$  as a function of the frequency,

$$\omega_{\mathbf{k}} = 2\sqrt{\sin^2(k_1/2) + \sin^2(k_2/2) + \sin^2(k_3/2)}, \quad (17)$$

on a  $32^3$  lattice after the equilibration process with the Langevin terms. We find that  $\langle |\pi(t, \mathbf{k})|^2 \rangle_{\text{eq}}$  is almost constant and is close to the given temperature,  $T = 1$ . By fitting a constant  $T_{\text{fit}}$  to  $\langle |\pi(t, \mathbf{k})|^2 \rangle_{\text{eq}}$ , we obtain,

$$T_{\text{fit}} = 1.002 \pm 0.007. \quad (18)$$

Thus the classical equilibrium is confirmed to be reached, where the measured temperature is consistent with the target one within the relative error of 0.2 %.

#### C. Time correlation of energy-momentum tensor

We shall now discuss the time correlation function  $C_{12}(t)$  of the energy-momentum tensor in the  $\phi^4$  theory. In Fig. 2, we show the time correlation of the energy-momentum tensor for several values of  $\lambda$  in the short time period,  $t < 5$ . In the time region of  $t < 5$ , the correlation seems to show damped oscillation around a constant value. The oscillation period is around  $\tau_{\text{short}} = 1.2 - 1.4$ . Then the frequency is evaluated as  $\omega_{\text{short}} = 2\pi/\tau_{\text{short}} \sim (4.5 - 5.2)$ .

By comparison, longer time results show that the background decreases especially at large  $\lambda$ , as shown in Fig. 3.

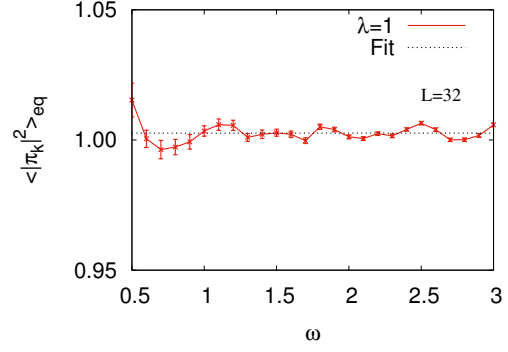


FIG. 1. Thermal expectation value of  $|\pi(t, \mathbf{k})|^2$ ,  $\langle |\pi(t, \mathbf{k})|^2 \rangle_{\text{eq}}$ , as a function of the lattice frequency  $\omega_{\mathbf{k}}$  on the  $32^3$  lattice after the thermalization process with the Langevin terms.

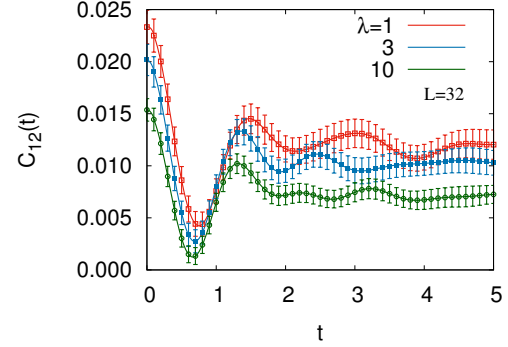


FIG. 2. The short time behavior ( $t < 5$ ) of the time correlation function of the energy momentum tensor,  $C_{12}(t) = V \langle \tau_{12}(t) \tau_{12}(0) \rangle$ , on the  $32^3$  lattice with the coupling  $\lambda = 1, 3$  and  $10$ .

We find that the correlation is found to oscillate around a slow monotonous decay. This slow decay may be approximated by an exponential function,

$$C_{12}^{(\text{exp})}(t) = A \exp(-\Gamma t). \quad (19)$$

We show the fit results using one exponential function by black dotted lines in Fig. 3, whose parameters are summarized in Table I, and their  $\lambda$  dependence is shown in Fig. 4. The fitting parameter  $A$  is not very sensitive to  $\lambda$ , while the  $\lambda$  dependence of  $\Gamma$  is strong. When we add a constant or another exponential term,  $\chi^2$  is slightly improved but the correlation among parameters makes parameter uncertainties much larger. Since  $C_{12}(t)$  should approach zero in the long time limit,  $t \rightarrow \infty$ , we assume that the decay is assumed to be given by the single exponential function in the later discussions.

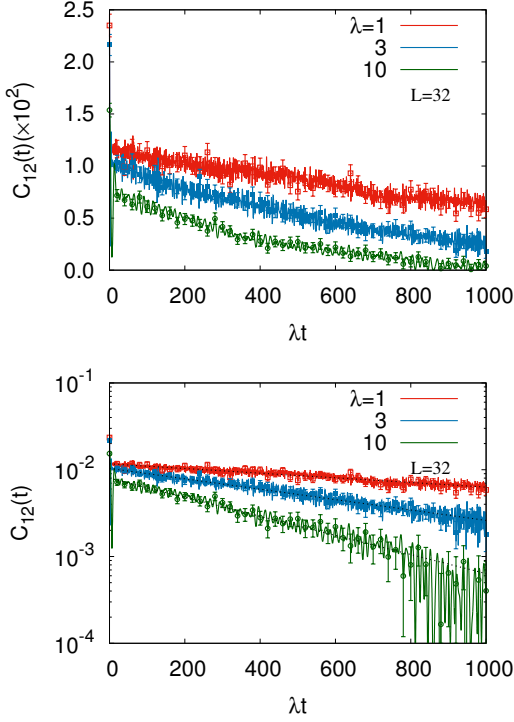


FIG. 3. Same as Fig. 2 but results in the long time range,  $\lambda t \leq 1000$ , are shown. In the upper and lower panels, we show the results in the linear and log scales, respectively. Black dotted lines show the single exponential functions, which fit the long time behavior.

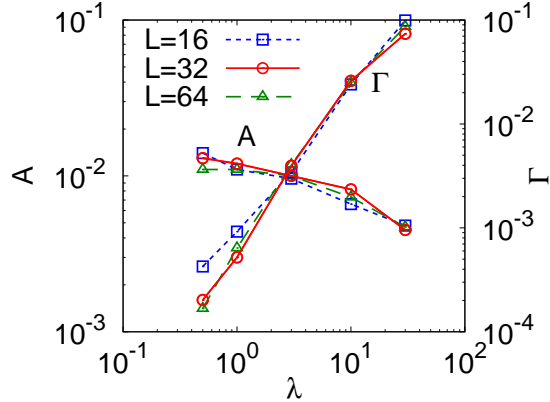


FIG. 4. The coupling dependence of  $(A, \Gamma)$ , where the time correlation function is fitted by the exponential function,  $C_{12}(t) \simeq A \exp(-\Gamma t)$ .

#### D. Fourier spectrum

Next, let us discuss the Fourier spectrum  $\rho(\omega)$  of the time correlation function of the energy-momentum ten-

TABLE I. Parameters in the exponential decay part of  $C_{12}(t)$  ( $A$  and  $\Gamma$ ) and the normalized shear viscosity ( $\lambda^2 \eta / T^3$ ) at  $\lambda = 0.5, 1, 3, 10$  and  $30$  on the  $16^3, 32^3$  and  $64^3$  lattices. We show the results at  $T = 1$ .

| $\lambda$ | $L$ | $A$                  | $\Gamma/\lambda^2$    | $\lambda^2 \eta / T^3$ |
|-----------|-----|----------------------|-----------------------|------------------------|
| 0.5       | 16  | $14 \times 10^{-3}$  | $17 \times 10^{-4}$   | 8.4                    |
|           | 32  | $13 \times 10^{-3}$  | $8.1 \times 10^{-4}$  | 16                     |
|           | 64  | $11 \times 10^{-3}$  | $6.7 \times 10^{-4}$  | 17                     |
| 1         | 16  | $11 \times 10^{-3}$  | $9.2 \times 10^{-4}$  | 12                     |
|           | 32  | $12 \times 10^{-3}$  | $5.2 \times 10^{-4}$  | 22                     |
|           | 64  | $11 \times 10^{-3}$  | $6.4 \times 10^{-4}$  | 17                     |
| 3         | 16  | $9.6 \times 10^{-3}$ | $3.8 \times 10^{-4}$  | 25                     |
|           | 32  | $10 \times 10^{-3}$  | $4.4 \times 10^{-4}$  | 23                     |
|           | 64  | $10 \times 10^{-3}$  | $4.5 \times 10^{-4}$  | 23                     |
| 10        | 16  | $6.6 \times 10^{-3}$ | $2.4 \times 10^{-4}$  | 27                     |
|           | 32  | $8.2 \times 10^{-3}$ | $2.6 \times 10^{-4}$  | 31                     |
|           | 64  | $7.3 \times 10^{-3}$ | $2.5 \times 10^{-4}$  | 29                     |
| 30        | 16  | $4.8 \times 10^{-3}$ | $1.1 \times 10^{-4}$  | 43                     |
|           | 32  | $4.5 \times 10^{-3}$ | $0.82 \times 10^{-4}$ | 54                     |
|           | 64  | $4.7 \times 10^{-3}$ | $0.96 \times 10^{-4}$ | 49                     |

sor,  $C_{12}(t)$ ,

$$\begin{aligned} \rho(\omega) &= \text{Re} \int_0^\infty dt e^{i\omega t} C_{12}(t) \\ &= \frac{1}{2} \left[ \int_0^\infty dt e^{i\omega t} C_{12}(t) + \int_{-\infty}^0 dt e^{i\omega t} C_{12}(-t) \right] \\ &\simeq \lim_{N \rightarrow \infty, \Delta t \rightarrow 0} \frac{\Delta t}{2} \sum_{n=-N/2+1}^{N/2} e^{i\omega n \Delta t} C_{12}(|n \Delta t|), \quad (20) \end{aligned}$$

where  $\Delta t = 2t_{\text{max}}/N$ . The last line in Eq. (20) is nothing but the discrete Fourier transformation, and we obtain the value of  $\rho(\omega)$  at  $\omega = n\pi/t_{\text{max}}$ . The zero frequency limit  $\lim_{\omega \rightarrow 0} \rho(\omega)$  is equal to the integral of  $C_{12}(t)$  to  $t = \infty$ , and is related with the shear viscosity as given in Eq. (24). The relation between the Fourier spectrum and the spectral density is described in Appendix C.

Integration up to  $t = \infty$  is not very easy. Since  $C_{12}(t)$  has a slow exponential decay part, we need  $C_{12}(t)$  at large  $t$ . As an example, we show the integral of  $C_{12}(t)$  to  $t$  in Fig. 5. At  $\lambda = 1$ , the decay rate  $\Gamma \simeq 5 \times 10^{-4}$  is small, and the integral is not yet saturated at  $\lambda t = 1000$  as shown by the lower dashed curve. At  $\lambda = 10$ , the integral is convergent but is still increasing at  $\lambda t = 1000$ . In order to avoid these problems, we first subtract the exponential decay part from  $C_{12}(t)$ , perform the integration, and add the Fourier transformation of the exponential decay part,  $A/\Gamma$ . With this prescription, the integral to  $t \rightarrow \infty$  is obtained efficiently even at a small value of  $t$  as shown by the open circles in Fig. 5.

The Fourier transformation is performed in a similar manner. We perform the Fourier transformation of the subtracted time correlation function  $C_{12}^{(\text{sub})}(t)$ , and the Fourier transformation of the exponential decay part is added after the discrete Fourier transformation in the



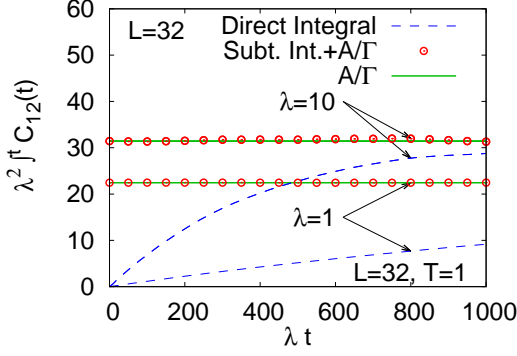


FIG. 5. Convergence of the integral of the time correlation function at  $\lambda = 1$  and  $10$  on the  $32^3$  lattice. The blue dashed lines show the naive integral results to  $t$ , while the open circles show the integrals of the subtracted correlation function,  $C_{12}^{(\text{sub})}(t) = C_{12}(t) - C_{12}^{(\text{exp})}(t)$ , to  $t$  plus the exponential decay contribution with  $t \rightarrow \infty$ ,  $A/\Gamma$ . The solid lines show  $A/\Gamma$ .

third line of Eq. (20),

$$\begin{aligned} \rho(\omega) &= \frac{1}{2} \text{F.T.}[C_{12}(t)] \\ &= \frac{1}{2} \left\{ \text{F.T.}[C_{12}^{(\text{sub})}(t)] + \text{F.T.}[C_{12}^{(\text{exp})}(|t|)] \right\}, \end{aligned} \quad (21)$$

$$C_{12}^{(\text{sub})}(t) = C_{12}(t) - C_{12}^{(\text{exp})}(|t|). \quad (22)$$

The exponential function in Eq. (19) contributes to the Fourier spectrum as a Lorentzian,

$$\rho^{(\text{exp})}(\omega) = \frac{1}{2} \text{F.T.}[C_{12}^{(\text{exp})}(|t|)] = \frac{A\Gamma}{\Gamma^2 + \omega^2}. \quad (23)$$

In Fig. 6, we show the Fourier spectra at  $\lambda = 1, 3$  and  $10$  on a  $32^3$  lattice. We find two structures, a peak at  $\omega = 0$  and a bump at  $\omega \simeq 4$ . At small  $\omega$ , the Fourier spectrum is dominated by the Lorentzian function from the slow decay part, shown by the dotted curves in the upper panel of Fig. 6. With decreasing  $\lambda$ , the decay rate  $\Gamma$  becomes smaller then the peak becomes sharper. The peak height of the zero frequency peak,  $A/\Gamma$ , has milder  $\lambda$  dependence.

At high frequencies, a broad bump appears around  $\omega = (2 - 6)$ . As already mentioned, the bump around  $\omega = 4$  produces the oscillatory behavior found in the early stage. This oscillation has mild dependence on  $\lambda$ , then it is natural to find similar shapes in the high frequency bumps. We fit the oscillation curves observed in  $C_{12}(t)$  in the early stage by three damped oscillators, and the Fourier transform of them are shown by dotted curves in the lower panel of Fig. 6.

This broad bump also appears in the free case,  $\lambda = 0$ . Then the frequency of  $C_{12}(t)$  should be given as the sum of frequencies of two momentum modes,  $\omega = \omega_{\mathbf{k}_1} + \omega_{\mathbf{k}_2}$ , in the free case. The single mode frequency is in the

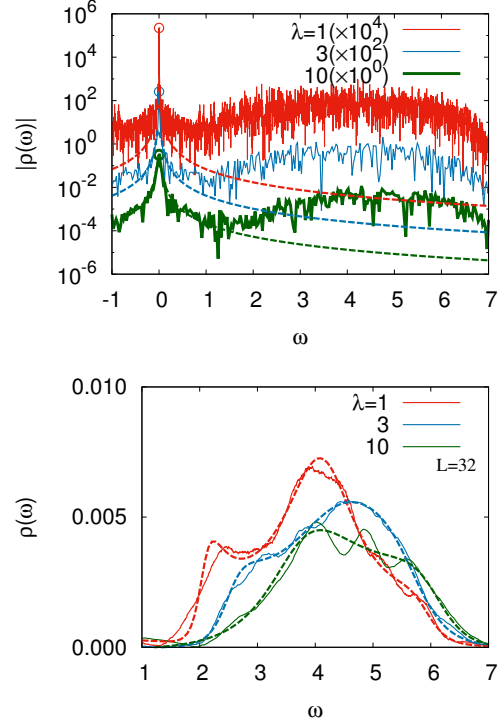


FIG. 6. Fourier spectra of the time correlation function,  $\rho(\omega)$ , on the  $32^3$  lattice with the coupling  $\lambda = 1$  (red),  $3$  (green) and  $10$  (blue). In the upper panel, we show  $\rho(\omega)$  in the log scale. Thin dashed curves show the Lorentzian functions, which are the Fourier transformations of the exponential decay parts. Thick dashed lines show the Fourier spectra, smeared by a Gaussian function with the standard deviation of  $\Delta\omega = 0.2$ . In the lower panel, we show  $\rho(\omega)$  in the high frequency region,  $\omega \geq 1$ . The smeared Fourier spectra are shown by solid curves. Dotted lines show the Fourier transform of the time correlation function, which fit the damped oscillation observed in the early stage.

range of  $0 \leq \omega_{\mathbf{k}} \leq 2\sqrt{3}$ , then the sum of two frequencies would be in the range  $0 \leq \omega \leq 4\sqrt{3} \simeq 7$  without the interaction, which agrees with the spread of the bump.

### E. Shear viscosity

By using the Fourier spectrum  $\rho(\omega)$ , the shear viscosity is obtained from the low-frequency limit,

$$\eta = \lim_{\omega \rightarrow 0} \frac{\rho(\omega)}{T}. \quad (24)$$

As already discussed, the Fourier transform of the exponential decay part of  $C_{12}(t)$  appears as a Lorentzian and dominates the Fourier spectrum at low frequencies. The contribution of the subtracted part is less than 1 % of the exponential decay part on a  $32^3$  lattice. Therefore, it is sufficient to consider the Lorentzian part in calculating the shear viscosity with a few percent accuracy. In this

approximation, the shear viscosity is found to be

$$\eta = \lim_{\omega \rightarrow 0} \frac{\rho(\omega)}{T} \simeq \lim_{\omega \rightarrow 0} \frac{\rho^{(\text{exp})}(\omega)}{T} = \frac{A}{T\Gamma}. \quad (25)$$

where  $A$  and  $\Gamma$  are the fitting parameters introduced in Eq. (19).

In characterizing the strength of the shear viscosity, the following “normalized” shear viscosity would be useful,

$$\bar{\eta} \equiv \frac{\lambda^2 \eta}{T^3} = \frac{\lambda^2 \eta_{\text{phys}}}{T_{\text{phys}}^3}. \quad (26)$$

From the dimensional considerations, the shear viscosity should be proportional to  $T_{\text{phys}}^3$ . The shear viscosity is proportional to the mean free path in rarefied gases, then the coupling dependence of  $\eta_{\text{phys}} \propto 1/\lambda^2$  is reasonable. Thus the combination  $\lambda^2 \eta_{\text{phys}}/T_{\text{phys}}^3$  is expected to depend on  $\lambda$  only weakly. Results of  $\lambda^2 \eta/T^3$  with  $T = 1$  are summarized in Table I.

While the actual numerical calculations are performed at  $T = 1$ , we can evaluate the shear viscosity with  $T \neq 1$  by using the  $\lambda$  deformation,  $\eta(\lambda/T, T) = T\eta(\lambda, T = 1)$ . Since  $\lambda T$  and  $\lambda\eta$  are invariant under the  $\lambda$  deformation, the normalized shear viscosity is found to be proportional to  $T^{-4}$  and sensitive to the choice of the lattice temperature  $T$ ,

$$\bar{\eta} = \frac{\lambda^2 \eta}{T^3} = \frac{(\lambda T)(\lambda \eta)}{T^4}. \quad (27)$$

We have set the cutoff as  $a^{-1}/T_{\text{phys}} = 0.2, 0.4$  and  $0.6$  based on the distribution function and the energy density as discussed in Appendix D.

In Fig. 7, we show the normalized shear viscosity  $\bar{\eta} = \lambda^2 \eta/T^3$  as a function of  $\lambda$  with the cutoff of  $a^{-1}/T_{\text{phys}} = 0.2, 0.4$  and  $0.6$ . We find small dependence of  $\bar{\eta}$  on  $\lambda$  as expected. While the shear viscosity measured on a  $16^3$  lattice is smaller at small  $\lambda$ , results on  $32^3$  and  $64^3$  lattices show similar values,  $\bar{\eta} \simeq 17 \times T^{-4}$ . With the choice of  $T^{-1} = 0.2, 0.4$  and  $0.6$ , the normalized shear viscosity is found to be around  $\bar{\eta} = 0.03, 0.4$  and  $2.2$ , respectively, at small  $\lambda$ . At large  $\lambda$ , lattice size dependence is found to be small, and  $\bar{\eta}$  increases slowly.

The shear viscosity of the  $\phi^4$  theory has been evaluated in perturbative calculations [10]. Their results show that the normalized shear viscosity is  $\lambda^2 \eta/T^3 = 733$  and  $2860$  at small  $\lambda$  in the one-loop and resummed calculations, and the normalized viscosity is an increasing function of  $\lambda$ . While the latter dependence agrees with the present results, the shear viscosity obtained from the classical field evolution is found to be smaller than the perturbative estimate.

By using the rarefied gas argument, the shear viscosity is proportional to the mean free path, then the above comparison suggests that the mean free path in the classical field theory is much shorter than that in perturbative calculations. The shorter mean free path in classical field theory may be reasonable, since the energy

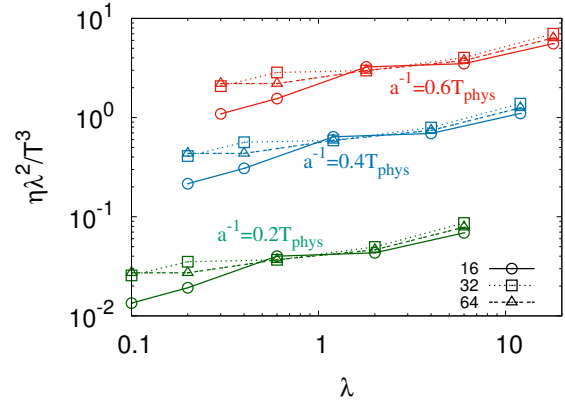


FIG. 7. The normalized shear viscosities,  $\bar{\eta} = \lambda^2 \eta/T^3$ , as functions of  $\lambda$  calculated on the  $16^3$ ,  $32^3$  and  $64^3$  lattices. The red, blue and green lines show the results with  $a^{-1}/T_{\text{phys}} = 0.2, 0.4$ , and  $0.6$ , respectively.

density spreads over all the lattice sites and each momentum mode always interacts with others in the classical field evolution. For example, the classical Yang-Mills field evolution seems to show smaller shear viscosity than the perturbation result [5].

It should be noted, however, that the valid momentum regions in the classical field treatment and in the perturbative treatment are different. Then, for a more serious estimate, it would be necessary to adopt frameworks, in which we can describe both of high and low momentum regions.

#### IV. SUMMARY

In this article, we have studied the shear viscosity of classical scalar fields on a lattice by using the classical field equation of motion, the Green-Kubo formula, and the classical field equilibrium configurations. Using the Green-Kubo formula, we can obtain the shear viscosity from the time correlation function of energy-momentum tensor in equilibrium. We have adopted the classical field ensemble method, where the classical field equilibrium configurations are generated by evolving the system with the artificial Langevin terms. We have confirmed the equilibrium is reached from the frequency dependence of the expectation value of the canonical momentum squared,  $\langle |\pi(\mathbf{k}, t)|^2 \rangle$ .

We have found that the time correlation function shows oscillatory behavior around a slow monotonous decay with an exponential form. The Fourier spectrum at low frequency is dominated by the slow decay, then the shear viscosity is also well evaluated by the contribution from the exponential decay. The calculated shear viscosity is found to be smaller than the perturbative results[10]. This may suggest the strong coupling feature of the low momentum regime for which the classical field

theory should be valid because each momentum mode always interacts with others in the time evolution.

The Fourier spectrum is found to have two components, a peak at  $\omega \simeq 0$  and a bump at  $\omega \simeq 4$ . The latter appears also in the free field theories. By comparison, the former comes from the slow exponential decay part and suggests that there exists a long-lived excitation mode, whose pole is on the imaginary axis,  $\omega = -i\Gamma$ . Since the damping rate is different from that of the high frequency peak by two or three orders, this long-lived mode should have the collective nature, such as the hydrodynamic modes.

While we have discussed the shear viscosity in the massless case ( $m = 0$ ), the dependence on the mass were discussed in Ref. [7]. It is interesting to examine the role of the slow decay also in finite mass and negative squared mass cases. It will be also valuable to discuss the shear viscosity of classical Yang-Mills field, which is considered to describe the initial stage of high-energy heavy-ion collisions. Another important direction to study is to include the quantum effects with the particle-field coupling and to describe short and long wave modes in a more consistent way.

#### Appendix A: Time correlation in free scalar theory with Langevin terms

It would be instructive to discuss the thermalization stage described by the Langevin equation. We show the time correlation function of the energy-momentum tensor,  $C_{12}(t) = V\langle\tau_{12}(t)\tau_{12}(0)\rangle$ , in the free scalar theory with the Langevin terms in Fig. 8. We set the parameters of the Langevin terms as ( $\gamma = 0.1, T = 1.0$ ). The red line shows  $C_{12}(t)$ , and the black line shows the fitting function. We find that  $C_{12}(t)$  damps exponentially while it slightly oscillates around the exponential decay part. We fit  $C_{12}(t)$  in the exponential function,  $C_{12}(t) = Ae^{-\Gamma t}$ , where fitting parameter  $A$  is the amplitude of the correlation function and  $\Gamma$  is the decay rate, which is the reciprocal of the relaxation time,  $\tau = \Gamma^{-1}$ . After the fitting, we obtain the set of fitting parameter,

$$\begin{aligned} A &= 0.01238 \quad +/ - 0.00003(0.2\%), \\ \Gamma &= 0.1061 \quad +/ - 0.0003(0.2\%). \end{aligned}$$

The decay rate is consistent with the diffusion coefficient,

$$\tau_{\text{rel}}^{-1} = \Gamma \sim \gamma. \quad (\text{A1})$$

Then the exponential damp of the correlation function is found to come from the diffusion term added in the Langevin equation, Eq. (9).

#### Appendix B: Analytic treatment of the time correlation function with Langevin terms

Let us consider the time correlation function of the free scalar theory with the Langevin terms in a model

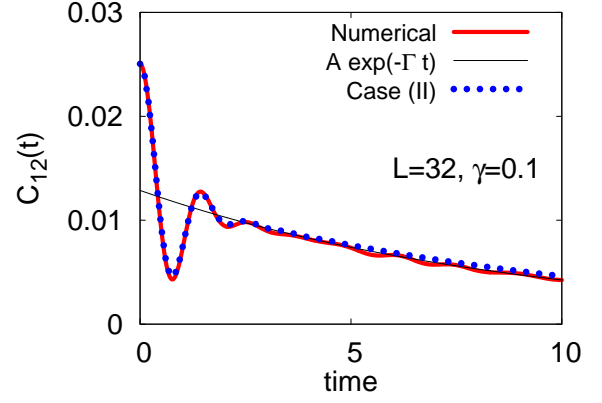


FIG. 8. The time correlation function  $C_{12}(t)$  of the free scalar theory with Langevin terms. We show the numerical calculation results on a  $32^3$  lattice with  $\gamma = 0.1$  and  $T = 1$ . As in the case with interaction,  $C_{12}(t)$  shows damped oscillation around the slow exponential decay. We also show the exponential function fitted to the numerical results (thin solid line) and the expected behavior from analytic calculation given in Appendix B (dotted line).

treatment. For preparation, let us recall the simplest Langevin equation,

$$\dot{p} = -\gamma p + R, \quad (\text{B1})$$

where  $R$  is a white noise,  $\langle R(t)R(t') \rangle = 2\gamma T\delta(t-t')$ . We can absorb the diffusion term by considering the combination,  $\exp(\gamma t)p(t)$ , then it is possible to integrate the equation of motion,

$$\frac{d}{dt}(e^{\gamma t}p) = e^{\gamma t}(\dot{p} + \gamma p) = e^{\gamma t}R(t), \quad (\text{B2})$$

$$p(t) = e^{-\gamma t} \left( p(0) + \int_0^t dt' e^{\gamma t'} R(t') \right). \quad (\text{B3})$$

Now let us apply the similar idea to the equation of motion of the free scalar theory together with the Langevin terms, which reduces to the Langevin equation for each momentum mode,

$$\dot{\pi}_{\mathbf{k}} = -\omega_{\mathbf{k}}^2 \phi_{\mathbf{k}} - \gamma \pi_{\mathbf{k}} + R_{\mathbf{k}}, \quad (\text{B4})$$

$$\dot{\phi}_{\mathbf{k}} = \pi_{\mathbf{k}}, \quad (\text{B5})$$

where  $R_{\mathbf{k}}$  is a complex white noise,  $\langle R_{\mathbf{k}}^*(t)R_{\mathbf{k}'}(t') \rangle = 2\gamma T\delta_{\mathbf{k}\mathbf{k}'}\delta(t-t')$ . By combining these equations, we obtain the equation of one variable  $X_{\mathbf{k}} = \pi_{\mathbf{k}} + i\Omega_{\mathbf{k}}\phi_{\mathbf{k}}$ , as in the simple Langevin equation,

$$\dot{X}_{\mathbf{k}} = i\bar{\Omega}_{\mathbf{k}}X_{\mathbf{k}} + R_{\mathbf{k}}, \quad (\text{B6})$$

$$\Omega_{\mathbf{k}} = \pm \bar{\omega}_{\mathbf{k}} - \frac{i}{2}\gamma, \quad (\text{B7})$$

$$\bar{\Omega}_{\mathbf{k}} = \Omega_{\mathbf{k}} + i\gamma = \pm \bar{\omega}_{\mathbf{k}} + \frac{i}{2}\gamma, \quad (\text{B8})$$

$$\bar{\omega}_{\mathbf{k}} = \sqrt{\omega_{\mathbf{k}}^2 - \gamma^2/4}. \quad (\text{B9})$$



We assume that  $\gamma$  is small enough,  $\gamma < \omega_{\mathbf{k}}/2$ , and  $\bar{\omega}_{\mathbf{k}}$  is real. Since the first equation (B6) reads

$$\frac{d}{dt} \left( e^{-i\bar{\omega}_{\mathbf{k}}t} X_{\mathbf{k}} \right) = e^{-i\bar{\omega}_{\mathbf{k}}t} R_{\mathbf{k}}, \quad (\text{B10})$$

then we can integrate the right hand side and get,

$$X_{\mathbf{k}}(t) = e^{i\bar{\omega}_{\mathbf{k}}t} \left[ X_{\mathbf{k}}(0) + \int_0^t dt' e^{-i\bar{\omega}_{\mathbf{k}}t'} R_{\mathbf{k}}(t') \right]. \quad (\text{B11})$$

In order to obtain  $\pi_{\mathbf{k}}$  and  $\phi_{\mathbf{k}}$  separately, we invoke the two solutions,  $\bar{\Omega}_{\mathbf{k}} = \pm \bar{\omega}_{\mathbf{k}} - i\gamma/2$ ,

$$\begin{aligned} (\pi_{\mathbf{k}} \pm i\bar{\omega}_{\mathbf{k}}\phi_{\mathbf{k}} + \frac{\gamma}{2}\phi_{\mathbf{k}})_t &= e^{\pm i\bar{\omega}_{\mathbf{k}}t - \gamma t/2} \\ &\times \left[ (\pi_{\mathbf{k}} \pm i\bar{\omega}_{\mathbf{k}}\phi_{\mathbf{k}} + \frac{\gamma}{2}\phi_{\mathbf{k}})_0 + \int_0^t dt' e^{\mp i\bar{\omega}_{\mathbf{k}}t' + \gamma t'/2} R_{\mathbf{k}}(t') \right]. \end{aligned} \quad (\text{B12})$$

By using these two, we find that  $\phi_{\mathbf{k}}(t)$  is given as the sum of the diffusion and fluctuation parts,

$$\phi_{\mathbf{k}}(t) = \phi_{\mathbf{k}}^D(t) + \phi_{\mathbf{k}}^F(t), \quad (\text{B13})$$

$$\begin{aligned} \phi_{\mathbf{k}}^D(t) &= e^{-\gamma t/2} \phi_{\mathbf{k}}(0) (\cos \bar{\omega}_{\mathbf{k}}t + \bar{\gamma} \sin \bar{\omega}_{\mathbf{k}}t) \\ &+ e^{-\gamma t/2} \frac{\pi_{\mathbf{k}}(0)}{\bar{\omega}_{\mathbf{k}}} \sin \bar{\omega}_{\mathbf{k}}t, \end{aligned} \quad (\text{B14})$$

$$\phi_{\mathbf{k}}^F(t) = \frac{1}{\bar{\omega}_{\mathbf{k}}} \int_0^t dt' R_{\mathbf{k}}(t') e^{-\gamma(t-t')/2} \sin \bar{\omega}_{\mathbf{k}}(t-t'), \quad (\text{B15})$$

where  $\bar{\gamma} = \gamma/2\bar{\omega}_{\mathbf{k}}$ .

The squared averages are calculated as

$$\begin{aligned} \langle \phi_{\mathbf{k}}^{F*}(t) \phi_{\mathbf{k}}^F(t) \rangle_{\text{eq}} &= \frac{2\gamma T}{\bar{\omega}_{\mathbf{k}}^2} \int_0^t dt' e^{-\gamma(t-t')/2} \sin^2 \bar{\omega}_{\mathbf{k}}(t-t') \\ &= \frac{T}{\bar{\omega}_{\mathbf{k}}^2} [1 - e^{-\gamma t} (1 + \bar{\gamma}^2 - \bar{\gamma}^2 \cos 2\bar{\omega}_{\mathbf{k}}t + \bar{\gamma} \sin 2\bar{\omega}_{\mathbf{k}}t)], \end{aligned} \quad (\text{B16})$$

$$\begin{aligned} \langle \phi_{\mathbf{k}}^{D*}(t) \phi_{\mathbf{k}}^D(t) \rangle_{\text{eq}} &= \frac{T e^{-\gamma t}}{\bar{\omega}_{\mathbf{k}}^2} [(\cos \bar{\omega}_{\mathbf{k}}t + \bar{\gamma} \sin \bar{\omega}_{\mathbf{k}}t)^2 + (1 + \bar{\gamma}^2) \sin^2 \bar{\omega}_{\mathbf{k}}t]. \end{aligned} \quad (\text{B17})$$

We now confirmed that the equilibrium value  $\langle \phi_{\mathbf{k}}^* \phi_{\mathbf{k}} \rangle_{\text{eq}} = T/\omega_{\mathbf{k}}^2$  is obtained at  $t \rightarrow \infty$  from the fluctuation part, Eq. (B16). Then in Eq. (B17) we have utilized this equilibrium value and that for  $\pi_{\mathbf{k}}$ ,  $\langle \pi_{\mathbf{k}}^*(0) \pi_{\mathbf{k}}(0) \rangle_{\text{eq}} = T$ .

For the later use, let us consider the average of four field product,  $\langle (\phi_{\mathbf{k}}^* \phi_{\mathbf{k}})^2 \rangle$ . We concentrate the fluctuation part, and we find that

$$\begin{aligned} \langle [\phi_{\mathbf{k}}^{F*}(t) \phi_{\mathbf{k}}^F(t)]^2 \rangle &= 2 \langle \phi_{\mathbf{k}}^{F*}(t) \phi_{\mathbf{k}}^F(t) \rangle^2 \\ &\rightarrow 2 \left( \frac{T}{\omega_{\mathbf{k}}} \right)^2. \end{aligned} \quad (\text{B18})$$

The factor 2 comes from the two ways of contractions, and the result looks natural. Nevertheless, readers may

care the product of four white noise terms. In order to be concrete, we express the white noise in a finite time step case,  $\int_{t_i}^{t_i+\Delta t} dt R_{\mathbf{k}}(t) = \sqrt{\gamma T \Delta t} \xi_i$  and  $\xi_i = \xi_i^R + i\xi_i^I$ , where  $\xi_i^R$  and  $\xi_i^I$  are random numbers in the  $i$ -th time step and obey the normal Gaussian distribution,

$$\begin{aligned} \langle \xi_i^R \xi_j^R \rangle &= \langle \xi_i^I \xi_j^I \rangle = \delta_{ij}, \quad \langle \xi_i^R \xi_j^I \rangle = 0, \\ \langle \xi_i^* \xi_j \rangle &= 2\delta_{ij}, \quad \langle \xi_i^* \xi_j^* \rangle = \langle \xi_i \xi_j \rangle = 0. \end{aligned} \quad (\text{B19})$$

Then some of the quartic average are given as

$$\langle (\xi_i^R)^4 \rangle = \langle (\xi_i^I)^4 \rangle = 3, \quad (\text{B20})$$

$$\langle (\xi_i^* \xi_i)^2 \rangle = \langle (\xi_i^R)^4 \rangle + 2 \langle (\xi_i^R)^2 \rangle \langle (\xi_i^I)^2 \rangle + \langle (\xi_i^I)^4 \rangle = 8, \quad (\text{B21})$$

$$\langle \xi_i^* \xi_j \xi_k^* \xi_\ell \rangle = 4(\delta_{ij} \delta_{k\ell} + \delta_{i\ell} \delta_{kj}). \quad (\text{B22})$$

It is interesting to find that there is no additional term appearing in the case of  $i = j = k = \ell$ . By using these relations, the quartic average of  $\phi$  is obtained as

$$\begin{aligned} &\langle [\phi_{\mathbf{k}}^{F*}(t) \phi_{\mathbf{k}}^F(t)]^2 \rangle \\ &= \int dt_1 dt_2 dt_3 dt_4 f(t_1) f(t_2) f(t_3) f(t_4) \\ &\quad \times \langle R_{\mathbf{k}}^*(t_1) R_{\mathbf{k}}(t_2) R_{\mathbf{k}}^*(t_3) R_{\mathbf{k}}(t_4) \rangle \\ &= (\gamma T \Delta t)^2 \sum_{i,j,k,\ell} f(t_i) f(t_j) f(t_k) f(t_\ell) \langle \xi_i^* \xi_j \xi_k^* \xi_\ell \rangle \\ &= 2 \left[ 2\gamma T \Delta t \sum_i f^2(t_i) \right]^2 = 2 \left[ 2\gamma T \int_0^t dt' f^2(t') \right]^2, \end{aligned} \quad (\text{B23})$$

where  $f(t') = e^{-\gamma(t-t')/2} \sin^2 \bar{\omega}_{\mathbf{k}}(t-t')/\bar{\omega}_{\mathbf{k}}$ .

We shall now evaluate the time correlation function. The spatial average of the energy-momentum tensor ( $xy$  element) is given as

$$\tau_{12} = \frac{1}{V} \sum_{\mathbf{x}} (\partial_1 \phi)(\partial_2 \phi) = \frac{1}{V} \sum_{\mathbf{k}} k_1 k_2 \phi_{\mathbf{k}}^* \phi_{\mathbf{k}}. \quad (\text{B24})$$

The time correlation function can be evaluated as

$$\begin{aligned} C_{12}(t) &= V \langle \tau_{12}(t) \tau_{12}(0) \rangle_{\text{eq}} \\ &= \frac{1}{V} \sum_{\mathbf{k}, \mathbf{k}'} k_1 k_2 k'_1 k'_2 \langle \phi_{\mathbf{k}}^*(t) \phi_{\mathbf{k}}(t) \phi_{\mathbf{k}'}^*(0) \phi_{\mathbf{k}'}(0) \rangle_{\text{eq}} \\ &= \frac{1}{V} \sum_{\mathbf{k}, \mathbf{k}'} k_1 k_2 k'_1 k'_2 [\langle \phi_{\mathbf{k}}^*(t) \phi_{\mathbf{k}}(t) \rangle_{\text{eq}} \langle \phi_{\mathbf{k}'}^*(0) \phi_{\mathbf{k}'}(0) \rangle_{\text{eq}} \\ &\quad + \langle \phi_{\mathbf{k}}^*(t) \phi_{\mathbf{k}'}(0) \rangle_{\text{eq}} \langle \phi_{\mathbf{k}'}^*(0) \phi_{\mathbf{k}}(t) \rangle_{\text{eq}} \\ &\quad + \langle \phi_{\mathbf{k}}^*(t) \phi_{\mathbf{k}'}^*(0) \rangle_{\text{eq}} \langle \phi_{\mathbf{k}'}(0) \phi_{\mathbf{k}}(t) \rangle_{\text{eq}}] \\ &= \frac{1}{V} \sum_{\mathbf{k}, \mathbf{k}'} k_1 k_2 k'_1 k'_2 C_\phi(\mathbf{k}, \mathbf{k}'; t) \\ &= \frac{2}{V} \sum_{\mathbf{k}} k_1^2 k_2^2 C_\phi(\mathbf{k}, \mathbf{k}; t), \end{aligned} \quad (\text{B25})$$

where the connected average  $C_\phi$  is given as

$$\begin{aligned}
C_\phi(\mathbf{k}, \mathbf{k}'; t) &= \langle \phi_{\mathbf{k}}^*(t) \phi_{\mathbf{k}}(t) \phi_{\mathbf{k}'}^*(0) \phi_{\mathbf{k}'}(0) \rangle_{\text{eq}} \\
&\quad - \langle \phi_{\mathbf{k}}^*(t) \phi_{\mathbf{k}}(t) \rangle_{\text{eq}} \langle \phi_{\mathbf{k}'}^*(0) \phi_{\mathbf{k}'}(0) \rangle_{\text{eq}} \\
&= \langle \phi_{\mathbf{k}}^*(t) \phi_{\mathbf{k}'}(0) \rangle_{\text{eq}} \langle \phi_{\mathbf{k}'}^*(0) \phi_{\mathbf{k}}(t) \rangle_{\text{eq}} \\
&\quad + \langle \phi_{\mathbf{k}}^*(t) \phi_{\mathbf{k}'}^*(0) \rangle_{\text{eq}} \langle \phi_{\mathbf{k}'}(0) \phi_{\mathbf{k}}(t) \rangle_{\text{eq}} \\
&= (\delta_{\mathbf{k}\mathbf{k}'} + \delta_{\mathbf{k}, -\mathbf{k}'}) \\
&\quad \times \langle \phi_{\mathbf{k}}^*(t) \phi_{\mathbf{k}}(0) \rangle_{\text{eq}} \langle \phi_{\mathbf{k}'}^*(0) \phi_{\mathbf{k}'}(t) \rangle_{\text{eq}}. \quad (\text{B26})
\end{aligned}$$

The equilibrium average of four field product factorizes as in the case of the Gaussian noise in Eq. (B22). Then, the contribution from the unconnected part,  $\langle \phi_{\mathbf{k}}^*(t) \phi_{\mathbf{k}}(t) \rangle_{\text{eq}} \langle \phi_{\mathbf{k}'}^*(0) \phi_{\mathbf{k}'}(0) \rangle_{\text{eq}}$ , in the third line of Eq. (B25) disappears, since the equilibrium distribution is isotropic and the equilibrium average of  $\tau_{12}$  in Eq. (B24) vanishes.

Then, by using the relation  $\phi_{-\mathbf{k}}(t) = \phi_{\mathbf{k}}^*(t)$ , the contributions from  $\mathbf{k}' = -\mathbf{k}$  as well as those from  $\mathbf{k}' = \mathbf{k}$  are found to survive, and we obtain the last line of Eq. (B25).

We find that only the diffusion part of  $\phi_{\mathbf{k}}(t)$  contribute to  $C_\phi$ , since the fluctuation part is independent of  $\phi_{\mathbf{k}}(0)$ .

$$\begin{aligned}
C_\phi(\mathbf{k}, \mathbf{k}'; t) &= e^{-\gamma t} (\cos \bar{\omega}_{\mathbf{k}} t + \bar{\gamma} \sin \bar{\omega}_{\mathbf{k}} t)^2 \\
&\quad \times [\langle (\phi_{\mathbf{k}}^* \phi_{\mathbf{k}})^2 \rangle_{\text{eq}} - \langle \phi_{\mathbf{k}}^* \phi_{\mathbf{k}} \rangle_{\text{eq}}^2] \\
&= e^{-\gamma t} \left( \frac{T}{\omega_{\mathbf{k}}^2} \right)^2 (\cos \bar{\omega}_{\mathbf{k}} t + \bar{\gamma} \sin \bar{\omega}_{\mathbf{k}} t)^2. \quad (\text{B27})
\end{aligned}$$

We have used the equilibrium average of the four field product,  $\langle (\phi_{\mathbf{k}}^* \phi_{\mathbf{k}})^2 \rangle_{\text{eq}} = 2(T/\omega_{\mathbf{k}}^2)^2$ . This value is different from that for the real variable obeying the Gaussian distribution. The time correlation function is now found to be

$$C_{12}(t) = \frac{2e^{-\gamma t}}{V} \sum_{\mathbf{k}} k_1^2 k_2^2 \left( \frac{T}{\omega_{\mathbf{k}}^2} \right)^2 (\cos \bar{\omega}_{\mathbf{k}} t + \bar{\gamma} \sin \bar{\omega}_{\mathbf{k}} t)^2. \quad (\text{B28})$$

Let us evaluate  $C_{12}(t)$  a little more in the Einstein-Debye treatment of the lattice momentum,  $1/V \times \sum_{\mathbf{k}} \rightarrow \int^\Lambda d\mathbf{k}/(2\pi)^3$ . We here ignore the diffusion effect on the oscillating frequency,  $\bar{\omega}_{\mathbf{k}} \rightarrow \omega_{\mathbf{k}} \simeq k$ . Then the time correlation function is evaluated as

$$\begin{aligned}
C_{12}(t) &\simeq 2T^2 e^{-\gamma t} \int^\Lambda \frac{d\mathbf{k}}{(2\pi)^3} \frac{k_1^2 k_2^2}{k^4} (\cos kt + \frac{\gamma}{2k} \sin kt)^2 \\
&= \frac{T^2 \Lambda^3 e^{-\gamma_c x}}{30\pi^2} [f_0(x) + 2\gamma_c f_1(x) + \gamma_c^2 f_2(x)], \quad (\text{B29})
\end{aligned}$$

$$f_0(x) = \frac{1}{3} + \frac{1}{x^3} ((x^2 - 2) \sin x + 2x \cos x), \quad (\text{B30})$$

$$f_1(x) = \frac{1}{x^2} (\sin x - x \cos x), \quad (\text{B31})$$

$$f_2(x) = 1 - \frac{\sin x}{x}, \quad (\text{B32})$$

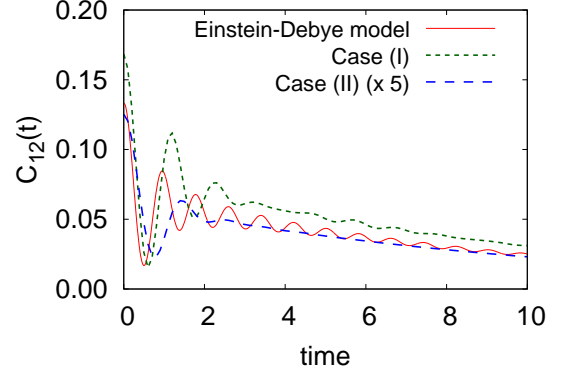


FIG. 9. The time correlation function  $C_{12}(t)$  in free scalar theory with Langevin terms at  $T = 1$  and  $\gamma = 0.1$ . In the Einstein-Debye model (solid curve), we take the cutoff  $\Lambda = (6\pi^2)^{1/3}$ . We also show the results with lattice momentum on a  $32^3$  lattice. In the case (I) (green dashed curve) and (II) (blue dotted curve), we adopt two ways of defining  $k_1$  and  $k_2$  (see the text).

where  $x = 2\Lambda t$  and  $\gamma_c = \gamma/2\Lambda$ .

In Fig. 9, we show  $C_{12}(t)$  in free scalar theory with Langevin terms. The qualitative behavior in the numerical results is well explained. We adopt the cutoff  $\Lambda = (6\pi^2)^{1/3}$ , which gives  $\int^\Lambda d\mathbf{k}/(2\pi)^3 = 1$ . We also show the results using the lattice momentum in Eq. (B28). We consider two cases of the lattice momentum. Case (I): We define the lattice momentum from the forward difference,  $k_i = 2 \sin(\pi n_i/L)$  ( $n_i = 0, 1, \dots, L-1$ ). Case (II): We use  $k_i = \sin(2\pi n_i/L)$  expected from the central difference. The latter results show smaller values of  $C_{12}(t)$ , and roughly agrees with the numerical calculation also in strength.

### Appendix C: Spectral density

We here briefly mention the relation of the Fourier spectrum and the spectral density. The spectral density  $\rho_{\text{den}}(\omega)$  is defined as the spectral function (Fourier spectrum) of the normal Green's function,  $\langle [\tau_{12}(t), \tau_{12}(0)] \rangle_{\text{eq}}$ . In general, the Fourier spectrum of the product and the spectral density are related for  $\omega \neq 0$ ,

$$\rho_{\text{den}}(\omega) \equiv \int dt e^{i\omega t} \langle [\tau_{12}(t), \tau_{12}(0)] \rangle_{\text{eq}}, \quad (\text{C1})$$

$$\begin{aligned}
I(\omega) &\equiv \int dt e^{i\omega t} \frac{1}{2} \langle \tau_{12}(t) \tau_{12}(0) \rangle_{\text{eq}} \\
&= \frac{1}{2} \coth \left( \frac{\omega}{2T} \right) \rho_{\text{den}}(\omega). \quad (\text{C2})
\end{aligned}$$

In the low frequency limit, this relation goes to the simple relation,

$$I(\omega) = \frac{T}{\omega} \rho_{\text{den}}(\omega).$$

Thus we can obtain the shear viscosity from the spectral density in the low frequency limit,  $\omega \rightarrow 0$  [9],

$$\eta = \lim_{\omega \rightarrow 0} \frac{VI(\omega)}{T} = \lim_{\omega \rightarrow 0} \frac{V\rho_{\text{den}}(\omega)}{\omega}.$$

In the main part of this article, we have used the Fourier spectrum  $\rho(\omega) = VI(\omega)$  instead of the spectral density  $\rho_{\text{den}}(\omega)$  for simplicity.

#### Appendix D: Choice of lattice spacing

In order to evaluate the shear viscosity in physical units, it is necessary to set the lattice spacing in physical units. As already discussed, we should take the cutoff  $a^{-1} = T_{\text{phys}}/T$  with the lattice temperature of  $T = \mathcal{O}(1)$ . We set the range of the lattice temperature  $T$  from the distribution function and the energy density of the Bose gas and the massless free classical fields.

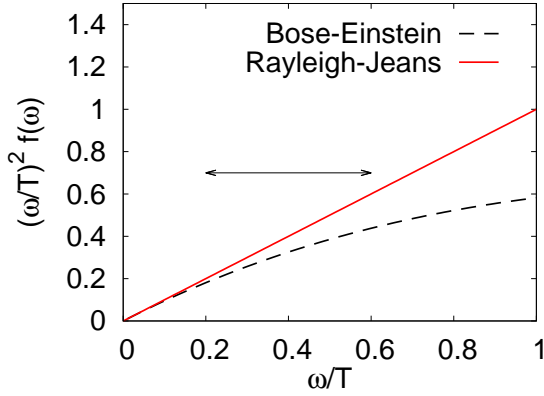


FIG. 10. Comparison of the Bose-Einstein distribution function (at  $\mu = 0$ ),  $f_{\text{BE}}(\omega) = (e^{\omega/T} - 1)^{-1}$ , and the Rayleigh-Jeans distribution function,  $f_{\text{RJ}}(\omega) = T/\omega$ , multiplied by  $(\omega/T)^2$ .

Comparison of the distribution functions prefers large values of the lattice temperature  $T$ . For the Bose gas, the distribution is given as the Bose-Einstein distribution,  $f_{\text{BE}}(\omega) = (e^{\omega/T} - 1)^{-1}$ . The massless free classical fields on the lattice obeys the Rayleigh-Jeans law and show the equipartition of energy, then the distribution function is interpreted as  $f_{\text{RJ}}(\omega) = T/\omega$ . In Fig. 10, we compare  $f_{\text{BE}}$  and  $f_{\text{RJ}}$  multiplied by  $(\omega/T)^2$ . It is found that two distribution functions are close in the low frequency region, and agree within the 10, 20, and 30 % differences for  $\omega/T = 0.2, 0.4$  and  $0.6$ , respectively, which confirms that classical field theory is an effective theory of quantum

field theory in the low frequency region. Note, however, that the frequency of the single particle mode extends to  $\omega_{\text{max}} = 2\sqrt{3}$  in the lattice unit, and  $f_{\text{RJ}}$  is larger than  $f_{\text{BE}}$  at  $\omega = \omega_{\text{max}}$  by 44, 116, and 236 % for  $1/T = 0.2, 0.4$  and  $0.6$ , respectively.

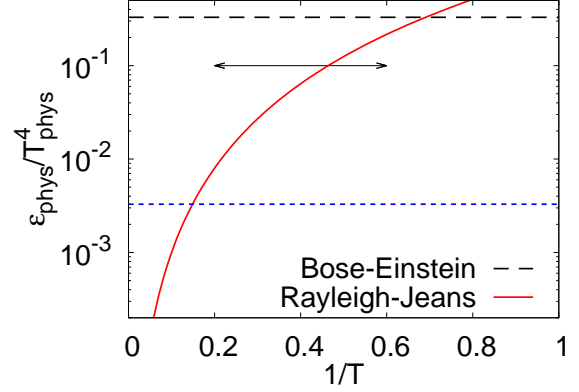


FIG. 11. Energy density normalized by  $T_{\text{phys}}^4$  of the Bose gas (dashed line) and the classical field (solid curve) as functions of  $1/T$ , where  $T$  is the lattice temperature. The dotted line shows 1 % of the Bose gas energy density.

By comparison, in order to take account of a significant part of the energy density of the Bose gas, relatively small lattice temperatures are preferred. The energy densities from  $f_{\text{BE}}$  and  $f_{\text{RJ}}$  are given as  $\epsilon_{\text{phys}}^{\text{EB}} = \pi^2 T_{\text{phys}}^4/30$  and  $\epsilon^{\text{RJ}} = E/L^3 = T(\epsilon_{\text{phys}}^{\text{RJ}} = T_{\text{phys}}^4/T^3)$ , respectively. In Fig. 11, we show these energy densities normalized by  $T_{\text{phys}}^4$  as functions of  $1/T$ . The Bose gas energy density is reproduced by choosing  $1/T = (\pi^2/30)^{1/3} \simeq 0.7$  in the massless free classical field. Since high frequency modes are ignored on the lattice, this value would be regarded as an upper bound. At  $1/T = 0.2, 0.4$  and  $0.6$ ,  $\epsilon_{\text{RJ}}/\epsilon_{\text{BE}} = 0.024, 0.19$  and  $0.66$ , respectively. When we choose a larger lattice temperature, say,  $1/T \lesssim 0.2$ , the classical field describes only a small fraction of the equilibrium energy density.

On the basis of these considerations, we set the lattice spacing in the range of  $a^{-1}/T_{\text{phys}} = 1/T = 0.2 \sim 0.6$  in Sec. III E. At  $1/T = 0.2$ ,  $f_{\text{BE}}$  and  $f_{\text{RJ}}$  agree within around 50% difference in the frequency range under consideration, while the energy density of the classical field is around 2.5% of the Bose gas. At  $1/T = 0.6$ , the energy density of the classical field is around 65% of that of the Bose gas, while the distribution function of the classical field overestimates that of the Bose gas by a factor of 3 at  $\omega = \omega_{\text{max}}$ . Since both of the distribution function and the energy density are important to discuss thermalization processes, we compare the results of the shear viscosity at  $1/T = 0.2, 0.4$  and  $0.6$ .

- [2] K. Sato, Mon. Notices Royal Astron. Soc. **195**, 467 (1981);  
A. H. Guth, Phys. Rev. D **23**, 347 (1981).
- [3] B. D. Serot and J. D. Walecka, Adv. Nucl. Phys. **16**, 1 (1986).
- [4] L. D. McLerran and R. Venugopalan, Phys. Rev. D **49**, 2233 (1994).
- [5] T. Epelbaum and F. Gelis, Phys. Rev. Lett. **111**, 232301 (2013).
- [6] B. Muller and A. Trayanov, Phys. Rev. Lett. **68**, 3387 (1992); T. S. Biro, C. Gong and B. Muller, Phys. Rev. D **52**, 1260 (1995); C. Gong, Phys. Rev. D **49**, 2642 (1994); J. Bolte, B. Muller and A. Schafer, Phys. Rev. D **61**, 054506 (2000); A. Dumitru, Y. Nara and M. Strickland, Phys. Rev. D **75**, 025016 (2007); T. Kunihiro, B. Muller, A. Ohnishi, A. Schafer, T. T. Takahashi and A. Yamamoto, Phys. Rev. D **82**, 114015 (2010); H. Iida, T. Kunihiro, B. Mueller, A. Ohnishi, A. Schafer and T. T. Takahashi, Phys. Rev. D **88**, 094006 (2013); H. Tsukiji, H. Iida, T. Kunihiro, A. Ohnishi and T. T. Takahashi, Phys. Rev. D **94**, 091502 (2016); H. Tsukiji, T. Kunihiro, A. Ohnishi and T. T. Takahashi, PTEP **2018**, 013D02 (2018).
- [7] M. M. Homor and A. Jakovac, Phys. Rev. D **92**, 105011 (2015).
- [8] D. N. Zubarev, V. Morozov, G. Röpke, *Statistical Mechanics of Nonequilibrium Processes, Volume 2 : Relaxation and Hydrodynamic Process* (Wiley-VCH, 1997).
- [9] J. I. Kapusta and C. Gale. *Finite-temperature field theory: Principles and applications* (Cambridge University Press, 2006).
- [10] S. Jeon, Phys. Rev. D **52**, 3591 (1995);  
S. Jeon and L. G. Yaffe, Phys. Rev. D **53**, 5799 (1996).
- [11] S. T. Cui, P. T. Cummings and H. D. Cochran, Molecular Physics **88**, 1657 (1996).
- [12] A. C. Brańka and D. M. Heyes, Phys. Rev. E **69**, 021202 (2004).